Crank Nicholson scheme to examine the fractional-order unsteady nanofluid flow of free convection of viscous fluids

Tamour Zubair[1]*, Muhammad Usman[2], Kottakkaran Sooppy Nisar[3], Ilyas Khan[4], Madiha Ghamkhar[5], Muhammad Ahmad[5]

1 School of Mathematical Sciences, Peking University, Beijing, China, 2 Department of Mathematics, National University of Modern Languages (NUML), Islamabad, Pakistan, 3 Department of Mathematics, College of Arts and Sciences, Wadi Aldawaser, Prince Sattam Bin Abdulaziz University, Al-Kharj, Saudi Arabia, 4 Department of Mathematics, College of Science Al-Zulfi, Majmaah University, Al-Majmaah, Saudi Arabia, 5 University of Agriculture, Faisalabad, Pakistan

* tamourzubair@pku.edu.cn

Abstract

Fractional fluid models are usually difficult to solve analytically due to complicated mathematical calculations. This difficulty in considering fractional model further increases when one considers nth order chemical reaction. Therefore, in this work an incompressible nanofluid flow as well as the benefits of free convection across an isothermal vertical sheet is examined numerically. An nth order chemical reaction is considered in the chemical species model. The specified velocity (wall's) is time-based, and its motion is translational into mathematical form. The fractional differential equations are used to express the governing flow equations (FDEs). The non-dimensional controlling system is given appropriate transformations. A Crank Nicholson method is used to find solutions for temperature, solute concentration, and velocity. Variation in concentration, velocity, and temperature profiles is produced as a result of changes in discussed parameters for both Ag-based and Cu-based nanofluid values. Water is taken as base fluid. The fractional-order time evaluation has opened the new gateways to study the problem into a new direction and it also increased the choices due to the extended version. It records the hidden figures of the problem between the defined domain of the time evaluation. The suggested technique has good accuracy, dependability, effectiveness and it also cover the better physics of the problem specially with concepts of fractional calculus.

1. Introduction

Natural convection process is that type of flow situation in which a liquid such as water as an example of Newtonian fluid, in which the fluid motion is produced by an external source instead by some parts of the fluid being heavier than other parts. More exactly, it is a specific kind of self-persistent flow with a high-temperature gradient, as a natural convection flow. This factor is then endorsed in order to get the non-uniform density. Because of changes in

density and gravitational field, buoyancy effects promote current movement. The aforementioned occurrences occur often in nature and have been documented in a variety of technical and engineering settings [1]. The most common model in convective flow models is natural convection, which involves the movement of heat and mass near a moving sheet. The aforementioned concept is often used in solar energy collectors, nuclear reactor architecture, and electronic devices. Various writers discussed the wonders of natural convection with the transfer of heat and mass, as well as the Newtonian/Non-Newtonian character of the fluid, due to its wide range of possible uses. The effect of convection (or free convection) on the accelerating plate in a perpendicular position was examined in [2], where they utilized the Laplace transformation technique (LTM) to examine the solution for two distinct circumstances, namely, the constant heat flux and isothermal plate. Refer to [3] for a free-convection flow issue in which a vertical plate is constructed in such a manner that it increases exponentially. Some of the prospective information may be examined methodically in references [4–11].

Following the contribution of Choi [12], the discipline of fluid mechanics received valuable concertation. Because he focused on thermal conductivity enrichment ideas related to fluids, he created the nano-fluids discipline. He demonstrated that nanoparticles, which are microscopic and small particles, may be put into fluids to convert them into nanofluids. The extensive research and experimental results revealed that it improves the thermal characteristics of the conventional fluid. As a result of this dramatic modernization, this area acquired considerable significance, and a large body of work is accessible in the literature. Sheikholelsami and Ganji [13] investigated the convective heat transport of nanofluids. [14–32] provide a comprehensive examination of nano-fluids and applications from different perspectives.

Previously, the fractional calculus theory sparked widespread interest due to its wide range of applications in physics and engineering [10]. This kind of research has made use of multidimensional dynamics such as wave, viscoelastic, and relaxation activities. Because of the operators, we developed a straightforward method for introducing fractional ordered derivatives into linear viscous models, which drew much attention to this area.

This research looked at the physical elements of the issue of fractional-order derivatives between certain domains. The fractional calculus makes visible contributions to various technical and scientific circumstances, including neurology, capacitor theory, viscoelasticity, electro-analytical chemistry, and electrical circuits [33,34]. Several authors [35–39] suggested several techniques for dealing with the nonlinearity of fractional differential equations. Despite the fact that there is extensive research literature on fluid flows, numerous mathematical and fluid models are developed and effectively solved using the fractional calculus method; see, for example, some useful investigations in this direction [7,40–42].

The above literature shows that several investigations are done on convection heat transfer using classical/fractional models [43–47] and [48–53]. However, in all these models, particularly those they are involved with fractional derivatives, no attention is given to nth order chemical reaction in species concentration and the free convection flow of viscous nanofluid using fractional derivatives. Therefore, the main objective of this work is to fill this gap. More exactly, in this article, water-based nanofluid is considered with Ag and Cu nanoparticles. The fractional differential equations are used to express the governing flow, heat, and species concentration equations. The Crank Nicholson technique is used to generate numerical results [54]. Variation in numerical implications of concentration, velocity, and temperature profiles is shown as a result of variations in various parameters for both Ag-based and Cu-based nanofluid values. The collected findings demonstrate the suggested technique's accuracy, dependability, and effectiveness.

2. Mathematical and geometrical analysis

Consider the mass and energy (heat) transmission performance of a nanofluid that is unsteady free convection, incompressible, one dimensional, viscous, and radiative, and is limited among specified plates that are parallel, filled with a porous material, and have distance d. Initially ($t = 0$), the fluid and plates are assumed to be stationary, and T_∞ and C_∞ are the constant temperature and constant concentration, respectively. For $t > 0$, the heat transfer process and surface temperature are proportionate. The nth-order chemical reaction is taken into account. Flow may be described using the following partial differential equations in light of the Boussinesq approximation.

$$\frac{\partial u}{\partial t} = v_{nf}\frac{\partial^2 u}{\partial y^2} + \frac{g}{\rho_{nf}}\beta_{nf}(T - T_\infty) + \frac{1}{\rho_{nf}}(\mathbf{J} \times \mathbf{B})_x - \frac{v_{nf}\phi_m}{k}u, \tag{1}$$

$$(\rho C_P)_{nf}\frac{\partial T}{\partial t} = k_{nf}\frac{\partial^2 T}{\partial y^2} - \frac{\partial q_r}{\partial y} \tag{2}$$

$$\frac{\partial C}{\partial t} = D\frac{\partial^2 C}{\partial y^2} + \gamma(C - C_\infty)^n, \tag{3}$$

Where $u(y, t)$, $T(y, t)$, $C(y, t)$, g, v_{nf}, ρ_{nf}, β_{nf}, σ_{nf}, $(C_P)_{nf}$, k_{nf} are the velocity, temperature, concentration gravitational acceleration, kinematics viscosity, density, heat transfer constant, electrical conductivity, heat capacity, and thermal conductivity. $\mathbf{J}$, D, γ, n and ϕ_m are the parameters for current density, mass diffusion, rate of chemical reaction, order of chemical reaction, and porosity, respectively.

$$v_{nf} = \frac{\mu_{nf}}{\rho_{nf}}, \mu_{nf} = \frac{\mu_f}{(1-\phi)^{2.5}}, \rho_{nf} = \rho_f\left((1-\phi) + \phi\frac{\rho_s}{\rho_f}\right), (\rho\beta)_{nf} = (1-\phi)(\rho\beta)_f +$$

$$\phi(\rho\beta)_s, \sigma_{nf} = \sigma_f\left(1 + \frac{3(\sigma-1)\phi}{\sigma+2-(\sigma-1)\phi}\right), \sigma = \frac{\sigma_s}{\sigma_f}, k_{nf} = k_f\frac{k_s + 2k_f - 2\phi\left(k_f - k_s\right)}{k_s + 2k_f + \phi\left(k_f - k_s\right)} \tag{4}$$

Where in Eqs (1)–(4), ρ_f, ρ_s, β_f, β_s, μ_{nf}, μ_f, σ_{nf}, σ_f, σ_s, k_f, k_s and ϕ are density, the density of solid particle, heat transfer constant, heat transfer constant for solid particle, viscosity, viscosity, viscosity of solid particle, electrical conductivity, the electrical conductivity of solid, thermal conductivity, thermal conductivity for solid, where the subscripts nf and f are for nanofluid and fluid, respectively. The current density value is

$$\mathbf{J} = \sigma_{nf}(E + \mathbf{V} \times \mathbf{B}), \tag{5}$$

where E is the electric field. Cogley et al. shows that [30]:

$$\frac{\partial q_r}{\partial y} = 4(T - T_\infty)\int_0^\infty k_{\lambda_w}\left(\frac{de_{b\lambda}}{dt}\right)_w d\lambda, \tag{6}$$

Where k_λ, $e_{b\lambda}$, w are the absorption coefficient, plank function and value at the wall $y = d$.

Substituting the values from Eqs (4–6) into Eqs (1–3), once obtained

$$\frac{\partial u}{\partial t} = v_{nf}\frac{\partial^2 u}{\partial y^2} + \frac{g}{\rho_{nf}}\beta_{nf}(T - T_\infty) - \frac{\sigma_{nf}B_0^2}{\rho_{nf}}u - \frac{v_{nf}\phi_m}{k}u, \tag{7}$$

$$(\rho c_P)_{nf}\frac{\partial T}{\partial t} = k_{nf}\frac{\partial^2 T}{\partial y^2} - 4(T - T_\infty)I, \tag{8}$$

$$\frac{\partial C}{\partial t} = D\frac{\partial^2 C}{\partial y^2} + \gamma(C - C_\infty)^n, \tag{9}$$

where $I = \int_0^\infty k_{\lambda_w}\left(\frac{de_{b\lambda}}{dt}\right)_w d\lambda$.

The associated initial and boundary conditions for Eqs (7)–(9) are:

$$u(y, 0) = 0, T(y, 0) = T_\infty, C(y, 0) = C_\infty.$$

for $t > 0$, $u(0, t) = u(1, t) = 0, \frac{\partial T}{\partial y}|_{y=0} = -\frac{1}{d}T(0, t), T(1, t) = T_\infty, C(0, t) = C_\infty, C(1, t) = C_w$.

To nondimensionalize the above system of PDEs let us consider the following transformations:

$$u = \frac{v_f}{d}\bar{u}, y = d\bar{y}, t = \frac{d^2}{v_f}\bar{t}, C = C_\infty\bar{C} + C_\infty, T = T_\infty\bar{T} + T_\infty,$$

Using the above transformation into (7–9), once obtained

$$\frac{\partial \bar{u}}{\partial \bar{t}} = \frac{1}{A(1 - \phi)^{2.5}}\frac{\partial^2 \bar{u}}{\partial \bar{y}^2} + \frac{BGr}{A}\bar{T} - \frac{M^2 C_1}{A}\bar{u} - \frac{N}{(1 - \phi)^{2.5}AD_1}\bar{u}, \tag{10}$$

$$EPr\frac{\partial \bar{T}}{\partial \bar{t}} = D_1\frac{\partial^2 \bar{T}}{\partial \bar{y}^2} - R\bar{T}, \tag{11}$$

$$\frac{\partial \bar{C}}{\partial \bar{t}} = \frac{1}{Le}\frac{\partial^2 \bar{C}}{\partial \bar{y}^2} + \delta\bar{C}^n, \tag{12}$$

Moreover A, B, C_1, D_1, E, F are just constants which introduced for simplicity and is given by:

$$A = \left((1 - \phi) + \phi\frac{\rho_s}{\rho_f}\right), B = \left((1 - \phi) + \frac{\phi(\rho\beta)_s}{(\rho\beta)_f}\right), C_1 = \left(1 + \frac{3(\sigma - 1)\phi}{\sigma + 2 - (\sigma - 1)\phi}\right),$$

$$D_1 = \frac{k_s + 2k_f - 2\phi\left(k_f - k_s\right)}{k_s + 2k_f + \phi\left(k_f - k_s\right)}, E = \left[(1 - \phi) + \phi\frac{\left(\rho c_p\right)_s}{\left(\rho c_p\right)_f}\right].$$

Transformed form of IC and BC's are given as:

$$\bar{u}(y,0) = \bar{T}(y,0) = \bar{C}(y,0) = 0,$$

$$\bar{u}(0,t) = 0, \frac{\partial \bar{T}}{\partial y}\bigg|_{y=0} = -\bar{T}(0,t) - 1, \bar{C}(0,t) = 0, \bar{u}(1,t) = 0, \bar{T}(1,t) = 0, \bar{C}(1,t) = 1.$$

The Caputo time fractional form of Eqs (8) and (9) are explained as follow also replacing $\bar{t}, \bar{y}, \bar{u}, \bar{T}$ and $\bar{C}$ by t, y, u, T and C:

$$D_t^\alpha u(y,t) = \frac{1}{A(1-\phi)^{2.5}}\frac{\partial^2 u}{\partial y^2} + \frac{BGr}{A}T - \frac{M^2 C_1}{A}u - \frac{N}{AD_1}u, \tag{13}$$

$$EPrD_t^\alpha T(y,t) = D_1\frac{\partial^2 T}{\partial y^2} - RT, \tag{14}$$

$$D_t^\alpha C(y,t) = \frac{1}{Le}\frac{\partial^2 C}{\partial \bar{y}^2} + \delta C^n. \tag{15}$$

where $D_t^\alpha V(y,t)$
$$\begin{cases} \dfrac{1}{\Gamma(1-\alpha)}\displaystyle\int_0^t \dfrac{1}{(t-\tau)^\alpha}\dfrac{\partial V(y,\tau)}{\partial \tau}d\tau, 0 < \alpha < 1, \\ \dfrac{\partial V(y,t)}{\partial t}, \alpha = 1. \end{cases}$$

3. Finite difference scheme

Crank Nicolson method (CNM) is projected to construct the numerical solution of problem (13–15) in this section. Consider the problem (13–15) for $n = 1$:

$$\frac{\partial^\alpha}{\partial t^\alpha}u(y,t) = \frac{1}{A(1-\phi)^{2.5}}\frac{\partial^2 u}{\partial y^2} + \frac{BGr}{A}T(y,t) - \frac{M^2 C_1}{A}u(y,t) - \frac{N}{AD_1}u(y,t), \tag{16}$$

$$E\ \mathrm{Pr}\frac{\partial^\alpha}{\partial t^\alpha}T(y,t) = D_1\frac{\partial^2 T}{\partial y^2} - RT(y,t), \tag{17}$$

$$D_t^\alpha C(y,t) = \frac{1}{Le}\frac{\partial^2 C}{\partial \bar{y}^2} + \delta C(y,t). \tag{18}$$

The boundary condition associated with above system given in above. In above $0 \le \alpha \le 1$ is Caputo derivative of fractional order. Consider that the above fractional-order system (16)–(18) has sufficiently smooth and has unique. Assume that $x_j = jh$, $0 \le j \le M$ with $Mh = 1$ and $t_n = n_\tau$, $0 \le n \le N$. Here h and τ indicate the space and time step length, M and N are represents the number of grids point. Fractional order derivate can discretize as [34]:

$$D_t^\alpha Q(y,t) = \frac{1}{\tau^\alpha \Gamma(2-\alpha)}\left[Q_j^{n+1} - Q_j^n + \sum_{i=1}^n \left(Q_j^{n-i+1} - Q_j^{n-i}\right)\left((i+1)^{1-\alpha} - i^{1-\alpha}\right)\right] + O(\tau),$$

and the second-order derivative using Crank-Nicholson idea can be discretized as under:

$$\frac{\partial^2}{\partial y^2} Q(y,t) = \frac{1}{2h^2}\left[\left(Q_{j+1}^{n+1} - 2Q_j^{n+1} + Q_{j-1}^{n+1}\right) + \left(Q_{j+1}^n - 2Q_j^n + Q_{j-1}^n\right)\right] + O(h^2).$$

Using the above-discretized formulas, system (16)–(18) takes the following form:

$$-\omega_{\tilde{u}}\tilde{u}_{j+1}^{n+1} + (\vartheta_{\tilde{u}} + 2\omega_{\tilde{u}})\tilde{u}_j^{n+1} - \omega_{\tilde{u}}\tilde{u}_{j-1}^{n+1}$$

$$= \omega_{\tilde{u}}\tilde{u}_{j+1}^n + \left(\vartheta_{\tilde{u}} - 2\omega_{\tilde{u}} - \left(\frac{M^2 C_1}{A} + \frac{N}{(1-\phi)^{2.5} A D_1}\right)\right)\tilde{u}_j^n + \omega_{\tilde{u}}\tilde{u}_{j-1}^n + \frac{BGr}{A}\tilde{T}_j^n$$

$$- \vartheta_{\tilde{u}}\sum_{i=1}^n \left(\tilde{u}_j^{n-i+1} - \tilde{u}_j^{n-i}\right)b_i,$$

$$-\omega_{\tilde{T}}\tilde{T}_{j+1}^{n+1} + (\vartheta_{\tilde{T}} + 2\omega_{\tilde{T}})\tilde{T}_j^{n+1} - \omega_{\tilde{T}}\tilde{T}_{j-1}^{n+1}$$

$$= \omega_{\tilde{T}}\tilde{T}_{j+1}^n + (\vartheta_{\tilde{T}} - 2\omega_{\tilde{T}} - R)\tilde{T}_j^n + \omega_{\tilde{T}}\tilde{T}_{j-1}^n - \vartheta_{\tilde{T}}\sum_{i=1}^n \left(\tilde{T}_j^{n-i+1} - \tilde{T}_j^{n-i}\right)b_i,$$

$$-\omega_{\tilde{C}}\tilde{C}_{j+1}^{n+1} + (\vartheta_{\tilde{C}} + 2\omega_{\tilde{C}})\tilde{C}_j^{n+1} - \omega_{\tilde{C}}\tilde{C}_{j-1}^{n+1}$$

$$= \omega_{\tilde{C}}\tilde{C}_{j+1}^n + (\vartheta_{\tilde{C}} - 2\omega_{\tilde{C}} + \delta)\tilde{C}_j^n + \omega_{\tilde{C}}\tilde{C}_{j-1}^n - \vartheta_{\tilde{C}}\sum_{i=1}^n \left(\tilde{C}_j^{n-i+1} - \tilde{C}_j^{n-i}\right)b_i,$$

where $\omega_{\tilde{u}} = \frac{1}{A(1-\phi)^{2.5}}\frac{1}{2h^2}, \vartheta_{\tilde{u}} = \frac{1}{\tau^\alpha \Gamma(2-\alpha)}, \omega_{\tilde{T}} = \frac{1}{2h^2}D_1, \vartheta_{\tilde{T}} = \frac{E\Pr}{\tau^\alpha \Gamma(2-\alpha)}, \omega_{\tilde{C}} = \frac{1}{Le}\frac{1}{2h^2},$

$$\vartheta_{\tilde{C}} = \frac{1}{\tau^\alpha \Gamma(2-\alpha)}, b_i = \left((i+1)^{1-\alpha} - i^{1-\alpha}\right).$$

$$\mathbf{A}_1\mathbf{v}^1 = \mathbf{B}\mathbf{v}^0 + \frac{BGr}{A}\mathbf{C}\mathbf{v}^0,$$

for $n \geq 1$,

$$\mathbf{A}_{n+1}\mathbf{v}^{n+1} = \mathbf{B}_{n+1}\mathbf{v}^n + \mathbf{s}_1^{n+1}\mathbf{v}^n + \mathbf{s}_2^{n+1}\mathbf{v}^{n-1} + \cdots + \mathbf{s}_n^{n+1}\mathbf{v}^1 + \mathbf{b}^{n+1}\mathbf{v}^0 + \frac{BGr}{A}\mathbf{C}\mathbf{v}^n.$$

In above $\mathbf{A}_{n+1}, \mathbf{B}_{n+1}, \mathbf{v}_n, \mathbf{s}_n^{n+1}, \mathbf{C}$ and $\mathbf{b}^{n+1}$ are represents the block matrices which are defined as follow:

$$\mathbf{A}_{n+1} = \begin{bmatrix} \mathbf{A}_{n+1}^{\tilde{u}} & \mathbf{O} & \mathbf{O} \\ \mathbf{O} & \mathbf{A}_{n+1}^{\tilde{T}} & \mathbf{O} \\ \mathbf{O} & \mathbf{O} & \mathbf{A}_{n+1}^{\tilde{C}} \end{bmatrix}, \mathbf{B}_{n+1} = \begin{bmatrix} \mathbf{B}_{n+1}^{\tilde{u}} & \mathbf{O} & \mathbf{O} \\ \mathbf{O} & \mathbf{B}_{n+1}^{\tilde{T}} & \mathbf{O} \\ \mathbf{O} & \mathbf{O} & \mathbf{B}_{n+1}^{\tilde{C}} \end{bmatrix}, \mathbf{C} = \begin{bmatrix} \mathbf{O} & \mathbf{I} & \mathbf{O} \\ \mathbf{O} & \mathbf{O} & \mathbf{O} \\ \mathbf{O} & \mathbf{O} & \mathbf{O} \end{bmatrix}, \mathbf{s}_n^{n+1}$$

$$= \begin{bmatrix} \mathbf{c}_n^T & \mathbf{O} & \mathbf{O} \\ \mathbf{O} & \mathbf{d}_n^T & \mathbf{O} \\ \mathbf{O} & \mathbf{O} & \mathbf{e}_n^T \end{bmatrix}^{n+1}, \mathbf{v}^n = \begin{bmatrix} \mathbf{u} \\ \mathbf{T} \\ \mathbf{C} \end{bmatrix}^n, \mathbf{b}^{n+1} = \begin{bmatrix} \mathbf{b}_n^T & \mathbf{O} & \mathbf{O} \\ \mathbf{O} & \mathbf{b}_n^T & \mathbf{O} \\ \mathbf{O} & \mathbf{O} & \mathbf{b}_n^T \end{bmatrix}^{n+1},$$

where the matrices $\mathbf{A}_{n+1}^{\tilde{u}}, \mathbf{A}_{n+1}^{\tilde{T}}, \mathbf{A}_{n+1}^{\tilde{C}}, \mathbf{B}_{n+1}^{\tilde{u}}, \mathbf{B}_{n+1}^{\tilde{T}}, \mathbf{B}_{n+1}^{\tilde{C}}, \mathbf{c}_n^T, \mathbf{d}_n^T, \mathbf{e}_n^T, \mathbf{I}$ and $\mathbf{b}_n^T$ present in [33,34] and

u and **T** are given as:

$$\mathbf{u}^n = \left[u_1^n, u_2^n, u_3^n, \ldots, u_{M-2}^n, u_{M-1}^n \right]^T,$$

$$\mathbf{T}^n = \left[T_1^n, T_2^n, T_3^n, \ldots, T_{M-2}^n, T_{M-1}^n \right]^T.$$

4. Discussion about numerical outcomes

The parametric study is provided to investigate the physics of the problem described in the preceding section. The fractional finite difference technique is used to find a numerical solution. Figs 1–11 show dimensionless velocity, temperature, and concentration plotted against the change of various parameters listed in Table 1.

Figs 1–5 depict the behaviour of velocity for water based nanofluid (with Prandtl number Pr = 6.2) containing copper (*Cu*) and silver (*Ag*) nanoparticles) for various values of fractional parameter α, as well as Hartmann number (*M*), porosity parameter (*N*), Grashof number (*Gr*), time (*t*) and solid volume fraction (ϕ) [43]. At time *t* = 0.3, the decreasing behaviour of velocity for Hartmann number (M^2) and fractional parameter α is shown in Fig 1.

M arises in the problem as a significance of substantial magnetic field effects, as is well known. As a consequence, magnetic forces working against the flow process become stronger, resulting in a decrease in velocity. Normally, this parameter causes the temperature to rise and the collision process to accelerate, which has a noticeable influence on the velocity, as seen in Fig 1. The fractional parameter stores the time evaluation values of velocity fluids, indicating that the velocity is steadily decreasing and nearing the fractional parameter's integer value. As a result, the fractional parameter traces the location of the fluid particles.

Fig 2 illustrates the effect of changing numerical values N and on velocity at *t* = 0.3. As the value of the porosity parameter is increased, the velocity impact diminishes (*N*). Increased porosity implies an increase in the degree of resistance. That is why the velocity of nanofluid decreases as the porosity parameter increases (*N*).
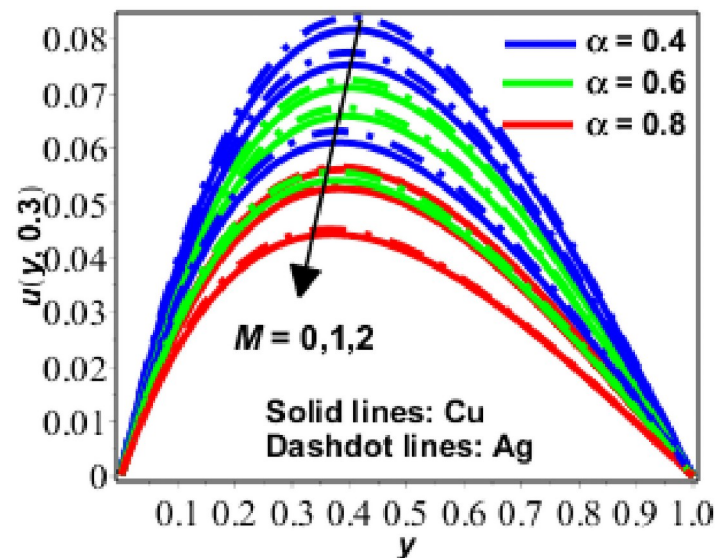

Fig 1. Variation in *u*(*y*, *t*) against *M* for Pr = 6.2, *Gr* = 0.9, *N* = 0.9, ϕ = 0.2, *R* = 0.9.
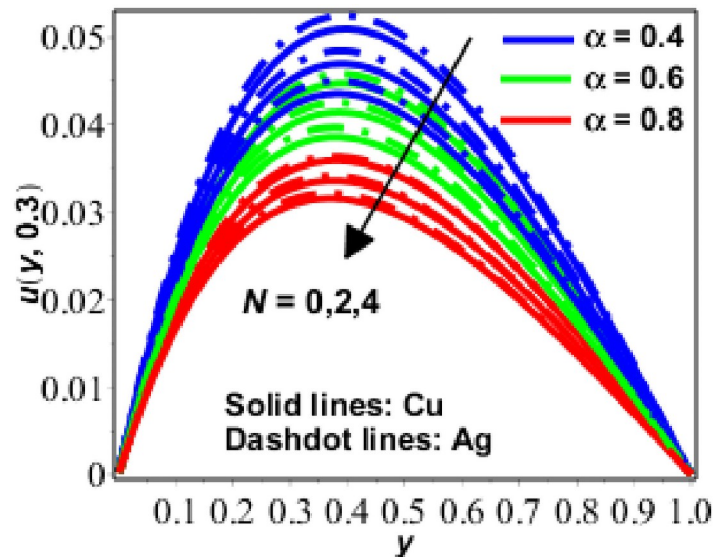
Fig 2. Variation in $u(y, t)$ against N for $Pr = 6.2$, $Gr = 0.9$, $M = 0.9$, $\phi = 0.2$, $R = 0.9$.

The effect of Gr on flow velocity is seen in Fig 3, which demonstrates that velocity increases as the size of *Gr* increases. As seen in the preceding section, the Grashof number is inversely related to the viscosity μ. Increased values of the Grashof number indicate that the viscosity is reducing, which explains why the velocity function is growing. Generally, an increase in any buoyancy-related parameter such as the Grashof number in the present case, causes an increase in the wall temperature, which weakens the bond(s) between the fluids, reduces internal friction pressure, and makes gravity stronger (i.e. makes the specific weight appreciably different between the immediate fluid layers adjacent to the wall). For detailed analysis of
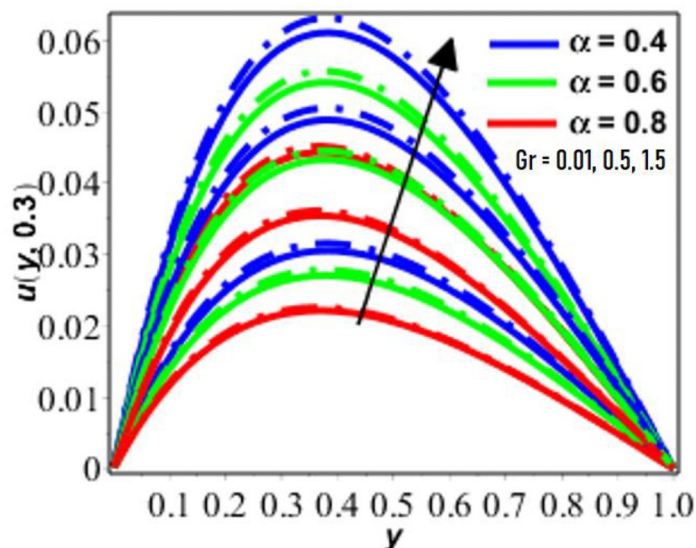

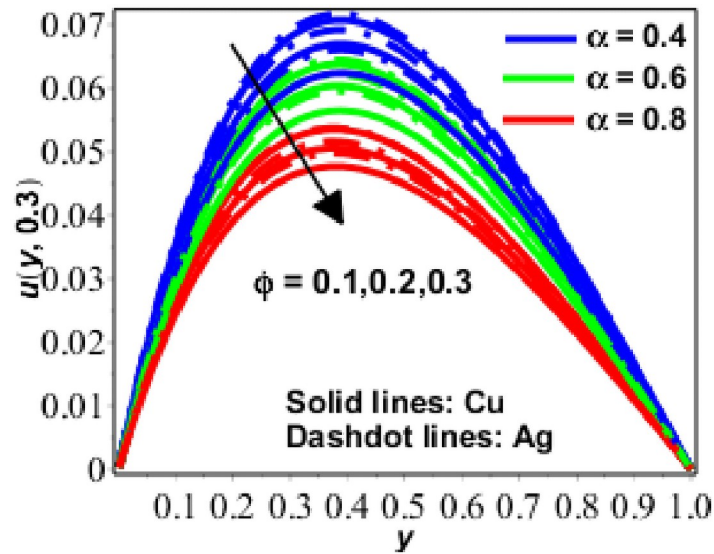**Fig 3. Variation in $u(y, t)$ against Gr for $Pr = 6.2$ $R = 0.9$, $M = 2$, $N = 0.2$, $\phi = 0.2$.**

Fig 4. Variation in $u(y, t)$ against R for Pr = 6.2 R = 0.5, Gr = 0.5, M = 2, N = 0.9.

https://doi.org/10.1371/journal.pone.0261860.g004

Grashof number and its effect on the fluid motion, three different scenarios (transport phenomenon) are discussed, namely: when (a) Grashof number is greater than 1, (b) Grashof number is less than 1, and (c) Grashof number is small (Gr = 0.01). In this first case, it is observed that velocity increases with increasing value of temperature-dependent viscosity parameter when Grashof number is greater than 1. In the second case, the observation showed that velocity decreases with increasing values of temperature-dependent viscosity parameter when Grashof number is less than 1. The third case examines the flow situation when the
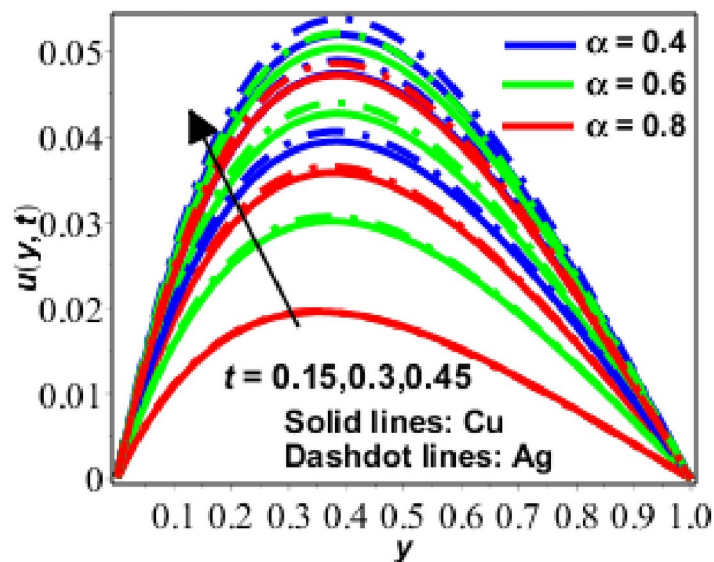

Fig 5. Variation in $u(y, t)$ against t for Gr = 0.5 R = 0.5, M = 2, N = 0.9, ϕ = 0.2, Pr = 6.2.

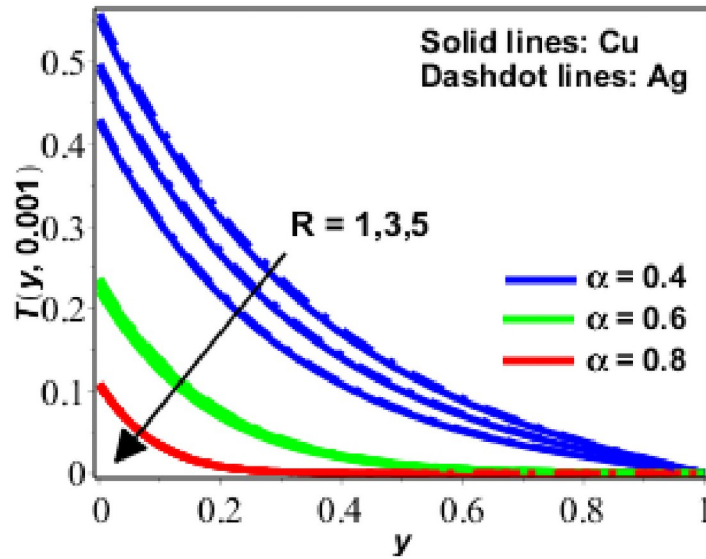https://doi.org/10.1371/journal.pone.0261860.g005

Fig 6. Behavior of $T(y, t)$ against R for Pr = 6.2 ϕ = 0.1.

when Grashof number is moderately small i.e. Gr = 0.01. The above observation shows that the Grashof number in convection flow plays and important role (Fig 3) [44,45].

Volume fraction is often used in solid materials science and engineering to refer to the concentration of a given phase, that is, the ratio of the volume of the particular phase to the total volume of the sample. Here in our study, ϕ shows the solid volume fraction of nanofluid. Additionally, Fig 4 has been displayed for various numerical values. As seen in Fig 4, velocity decreases as the numerical value of for nanofluid increases. In Fig 5, the velocity behaviour for changing t has been illustrated, demonstrating that flow velocity steadily increases with time.
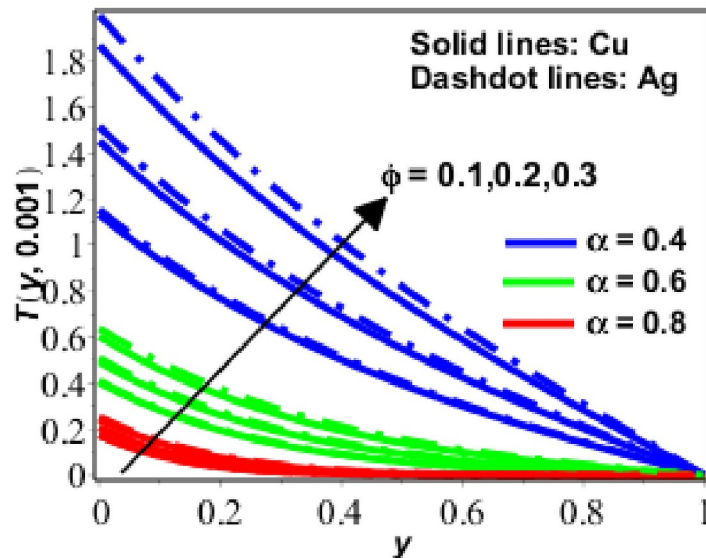

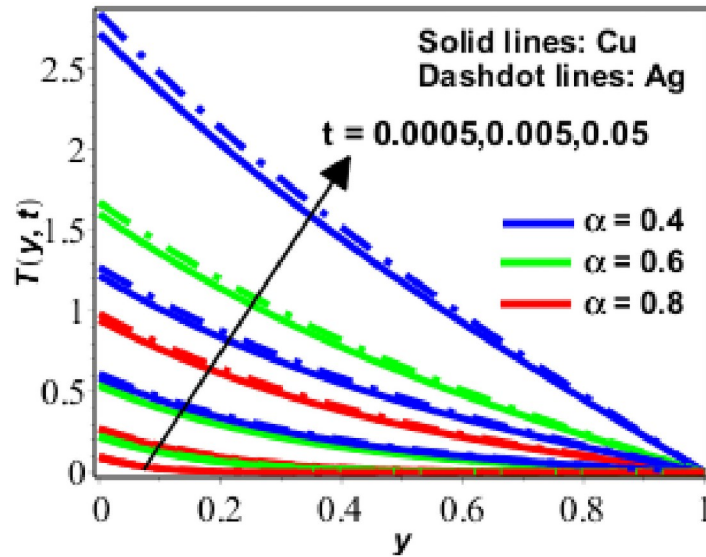**Fig 7. Behavior of $T(y, t)$ against ϕ for Pr = 6.2.**

Fig 8. Variation in $T(y, t)$ against t for $R = 0.1$ $\phi = 0.1$, Pr = 6.2.

The temperature performance of nanofluids (based on copper (Cu) and silver (Ag)) has been presented in Figs 6–9 for various numerical parameter values and fractional parameter values. Fig 6 demonstrates that the temperature of the nanofluid decreases as the radiation effects N increase, indicating that the nanofluid is radiative in nature and radiates energy. As a result of this, radiation (in the form of electromagnetic waves) wastes energy, reducing the thickness of the thermal boundary layer and therefore the temperature. The temperature increases as the value of the solid volume fraction (ϕ) disclosed in Fig 7 which is increased. In Fig 8, a similar response of the temperature of the nanofluid was seen when the numerical
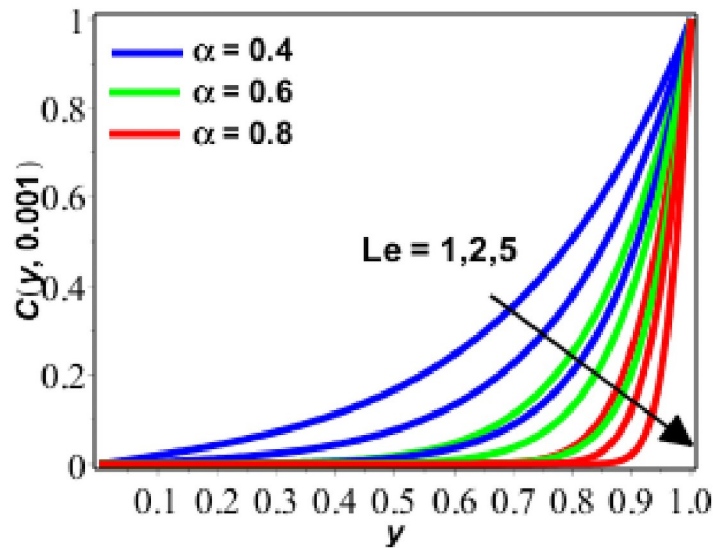

Fig 9. Behavior of $C(y, t)$ against Le for $\delta = 0.9$.
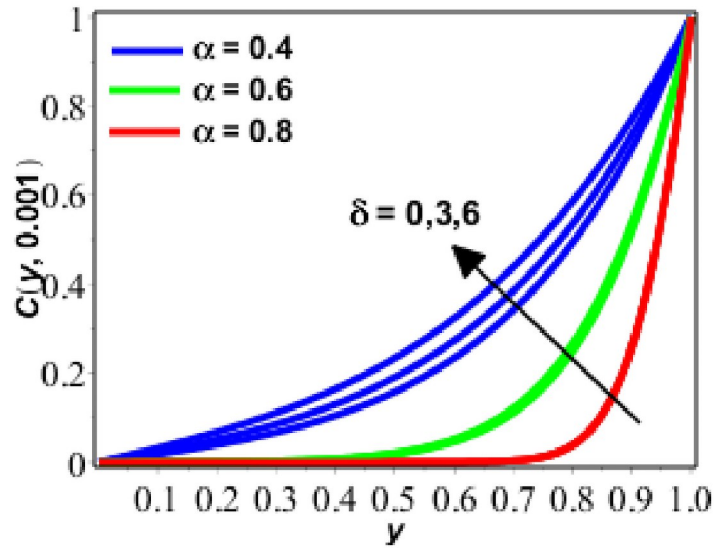
Fig 10. Variation in $C(y, t)$ against δ for $Le = 1$.

values t and α were changed. Moreover, as seen in Fig 8, nano fluids based on silver have a greater temperature than nano fluids based on copper.

Enactment of concentration of solute is presented on Figs 9–11 for diverse values of parameters. Figs 9 and 10 show the performance of concentration of solute for upsurging numerical values of Lewis number (Le) and δ. Fig 9 shows that concentration and concentration boundary layer thickness is decreeing as we are increasing the magnitude of Le. The motive behind is that when the Le increases, the diffusion process decreases because of the inversely proportional relationship between Le and diffusion. As the diffusion process decreases, the

Fig 11. Behavior of $C(y, t)$ against t for $\delta = 0.9$ $Le = 2$.

Table 1. The expressions of parameters used in Eqs (10)–(12) are given in tabular form.

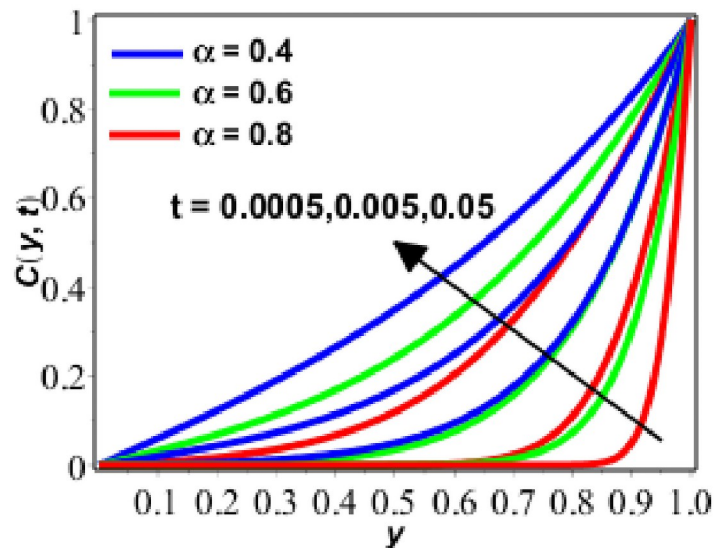| Parameter	Expression	Parameter	Expression
Grashof number	$Gr = \frac{g\beta_f\left(T_w - T_\infty\right)d^3}{v_f^2}$	Prandtl number	$\Pr = \frac{\mu_f(c_P)_f}{k_f}$
Hartmann number	$M^2 = \frac{\sigma B_0^2 d^2}{\mu_f}$	Radiation	$R = \frac{4Id^2}{k_f}$
Porosity	$N = \frac{d^2\phi_m}{k_f}$	Lewis number	$Le = \frac{v_f}{D}$
Reaction rate	$\delta = \frac{\gamma d^2(C_w - C_\infty)^{n-1}}{v_f}$	Fractional	α

concentration of solute is also decreased. On the other hand, the response rate parameter exhibits the inverse relationship. In this situation, we can readily assert that the rate of chemical reaction rises as the reaction rate parameter increases. This becomes the cause for the growing behaviour of the solute's concentration. In Fig 10, the concentration of solute increases with increasing δ and decreases with increasing fractional parameter. In the last Fig 11, the concentration of solute increases with the passage of time and with the decreasing values of the fractional parameter (α).

5. Conclusion

The viscous, incompressible, and convection-free fluidic flow near an isothermal vertical plate is theoretically investigated in this article. The plate's velocity varies with time, and its motion is translational. The fractional differential equations are used to express the governing flow equations (FDEs). A mixture of finite difference and Crank Nicolson techniques is used to find numerical solutions for solute concentration, velocity, and temperature. As a result, the following is the main summary of our research:

- The outlines of temperature, velocity, and concentration reduced, while the total numerical values of parameter α decreased.

- Values for velocity and temperature for the case of Ag-based nanofluid is more than Cu-based nanofluid

- Ordinary fluid flow is more leisurely than fractional fluid flow.

- The velocity, temperature, and concentration profiles all showed declining behaviour as time passed.

Supporting information

S1 Abbreviations.
(DOCX)

Author Contributions

Conceptualization: Tamour Zubair, Madiha Ghamkhar.

Data curation: Muhammad Usman, Kottakkaran Sooppy Nisar.

Formal analysis: Ilyas Khan, Muhammad Ahmad.

Investigation: Tamour Zubair, Muhammad Usman, Muhammad Ahmad.

Methodology: Muhammad Usman.

Resources: Kottakkaran Sooppy Nisar.

Software: Kottakkaran Sooppy Nisar.

Validation: Tamour Zubair, Ilyas Khan, Muhammad Ahmad.

Visualization: Muhammad Usman.

Writing – review & editing: Tamour Zubair.

References

1. P. GHOSHDASTIDAR, "Ghoshdastidar, PS Ghoshdastidar-heat Transfer-oxford University Press (2012). pdf," *pdfcookie.com*.

2. Gupta A., "Free convection effects on the flow past an accelerated vertical plate in an incompressible dissipative fluid," 1979.

3. Singh A. K. and Kumar N., "Free-convection flow past an exponentially accelerated vertical plate," *Astrophys. Space Sci.*, vol. 98, no. 2, pp. 245–248, Jan. 1984, https://doi.org/10.1007/BF00651403

4. Merkin J. H., "A note on the similarity solutions for free convection on a vertical plate," *J. Eng. Math.*, vol. 19, no. 3, pp. 189–201, Sep. 1985, https://doi.org/10.1007/BF00042533

5. N. Roşca, A. Roşca, I. P.-C. & mathematics with applications, and undefined 2016, "Lie group symmetry method for MHD double-diffusive convection from a permeable vertical stretching/shrinking sheet," *Elsevier*.

6. Toki C. J. and Tokis J. N., "Exact solutions for the unsteady free convection flows on a porous plate with time-dependent heating," *ZAMM Zeitschrift fur Angew. Math. und Mech.*, vol. 87, no. 1, pp. 4–13, Jan. 2007, https://doi.org/10.1002/ZAMM.200510291

7. Toki C. J., "Unsteady free-convection flow on a vertical oscillating porous plate with constant heating," *J. Appl. Mech. Trans. ASME*, vol. 76, no. 1, pp. 1–4, 2009.

8. V. R. -I . J. of A. M. and Mech and undefined 2010, "MHD effects on free convection and mass transform flow through a porous medium with variable temperature," *researchgate.net*, vol. 6, no. 14, pp. 1–16, 2010.

9. Narahari M. and Ishak A., "Radiation effects on free convection flow near a moving vertical plate with newtonian heating," *J. Appl. Sci.*, vol. 11, no. 7, pp. 1096–1104, 2011, https://doi.org/10.3923/JAS.2011.1096.1104

10. Rubbab Q., Vieru D., Fetecau C., and Fetecau C., "Natural convection flow near a vertical plate that applies a shear stress to a viscous fluid," *PLoS One*, vol. 8, no. 11, Nov. 2013, https://doi.org/10.1371/JOURNAL.PONE.0078352 PMID: 24278110

11. A. Khalid, I. Khan, A. Khan, S. S.-E. S. and Technology, and undefined 2015, "Unsteady MHD free convection flow of Casson fluid past over an oscillating vertical plate embedded in a porous medium," *Elsevier*.

12. S. Choi and J. Eastman, "Enhancing thermal conductivity of fluids with nanoparticles," 1995.

13. M. Sheikholeslami, D. G.-J. of the T. I. of Chemical, and undefined 2016, "Nanofluid convective heat transfer using semi analytical and numerical approaches: a review," *Elsevier*.

14. M. Usman, M. Hamid, U. Khan, S. Din, . . . M. I.-A. engineering, and undefined 2018, "Differential transform method for unsteady nanofluid flow and heat transfer," *Elsevier*.

15. U. Khan, N. Ahmed, S. Khan, S. M.-P. and Power, and undefined 2014, "Thermo-diffusion effects on MHD stagnation point flow towards a stretching sheet in a nanofluid," *Elsevier*.

16. KIM J., KANG Y. T., and CHOI C. K., "Analysis of convective instability and heat transfer characteristics of nanofluids," *Phys. FLUIDS*, vol. 16, pp. 2395–2401, 2004.

17. Khan M. S., Karim I., Ali L. E., and Islam A., "Unsteady MHD free convection boundary-layer flow of a nanofluid along a stretching sheet with thermal radiation and viscous dissipation effects," *Int. Nano Lett.*, vol. 2, no. 1, Dec. 2012, https://doi.org/10.1186/2228-5326-2-24

18. Kumar A., Sugunamma V., and Sandeep N., "Impact of Non-linear Radiation on MHD Non-aligned Stagnation Point Flow of Micropolar Fluid over a Convective Surface," *J. Non-Equilibrium Thermodyn.*, vol. 43, no. 4, pp. 327–345, Oct. 2018.

19. M. Usman, R. Haq, M. Hamid, W. W.-J. of M. Liquids, and undefined 2018, "Least square study of heat transfer of water based Cu and Ag nanoparticles along a converging/diverging channel," *Elsevier*.

20. Mohyud-Din S. T., Usman M., Afaq K., Hamid M., and Wang W., "Examination of carbon-water nanofluid flow with thermal radiation under the effect of Marangoni convection," *Eng. Comput. (Swansea, Wales)*, vol. 34, no. 7, pp. 2330–2343, 2017.

21. F. Garoosi, L. Jahanshaloo, . . . M. R.-A. M., and undefined 2015, "Numerical simulation of natural convection of the nanofluid in heat exchangers using a Buongiorno model," *Elsevier*.

22. M. S.-P. L. A and undefined 2017, "Numerical simulation of magnetic nanofluid natural convection in porous media," *Elsevier*.

23. Khan U., Ahmed N., Mohyud-Din S. T., and Bin-Mohsin B., "Nonlinear radiation effects on MHD flow of nanofluid over a nonlinearly stretching/shrinking wedge," *Neural Comput. Appl.*, vol. 28, no. 8, pp. 2041–2050, Aug. 2017, https://doi.org/10.1007/S00521-016-2187-X

24. B. Ankamwar, "Chapter 4 Size and Shape Effect on Biomedical Applications of Nanomaterials," 2012.

25. Raza M. A., Kanwal Z., Rauf A., Sabri A. N., Riaz S., and Naseem S., "Size- and Shape-Dependent Antibacterial Studies of Silver Nanoparticles Synthesized by Wet Chemical Routes," *Nanomaterials*, vol. 6, no. 4, Apr. 2016, https://doi.org/10.3390/nano6040074 PMID: 28335201

26. Ashwinkumar G. P., Samrat S. P., and Sandeep N., "Convective heat transfer in MHD hybrid nanofluid flow over two different geometries," *Int. Commun. Heat Mass Transf.*, vol. 127, p. 105563, Oct. 2021, https://doi.org/10.1016/J.ICHEATMASSTRANSFER.2021.105563

27. S. Samrat, G. Ashwinkumar, and N. Sandeep, "Simultaneous solutions for convective heat transfer in dusty-nano- and dusty-hybrid nanoliquids:," https://doi.org/10.1177/09544089211043605, p. 095440892110436, Sep. 2021.

28. Ashwinkumar G. P., "Heat and mass transfer analysis in unsteady MHD flow of aluminum alloy/silver-water nanoliquid due to an elongated surface," *Heat Transf.*, vol. 50, no. 2, pp. 1679–1696, Mar. 2021, https://doi.org/10.1002/HTJ.21947

29. F. Mabood, G. P. Ashwinkumar, and N. Sandeep, "Effect of nonlinear radiation on 3D unsteady MHD stagnancy flow of Fe3O4/graphene–water hybrid nanofluid," *https://doi.org/10.1080/01430750.2020. 1831593*, 2020.

30. Chalavadi S., Madde P., Naramgari S., and Poojari A. G., "Effect of variable heat generation/absorption on magnetohydrodynamic Sakiadis flow of Casson/Carreau hybrid nanoliquid due to a persistently moving needle," *Heat Transf.*, 2021, https://doi.org/10.1002/HTJ.22280

31. Mabood F., Ashwinkumar G. P., and Sandeep N., "Simultaneous results for unsteady flow of MHD hybrid nanoliquid above a flat/slendering surface," *J. Therm. Anal. Calorim. 2020 1461*, vol. 146, no. 1, pp. 227–239, Jun. 2020, https://doi.org/10.1007/S10973-020-09943-X

32. Tlili I., Nabwey H. A., Ashwinkumar G. P., and Sandeep N., "3-D magnetohydrodynamic AA7072-AA7075/methanol hybrid nanofluid flow above an uneven thickness surface with slip effect," *Sci. Reports 2020 101*, vol. 10, no. 1, pp. 1–13, Mar. 2020, https://doi.org/10.1038/s41598-020-61215-8 PMID: 32144369

33. V. Kulish, J. L.-J. F. Eng., and undefined 2002, "Application of fractional calculus to fluid mechanics," *asmedigitalcollection.asme.org*.

34. Rostami Y., "Operational matrix of two dimensional Chebyshev wavelets and its applications in solving nonlinear partial integro-differential equations," *Eng. Comput. (Swansea, Wales)*, vol. 38, no. 2, pp. 745–761, Feb. 2021.

35. Ahmed N., Khan U., Khan S., . . . Y. X.-J.-. . . J. of P., and undefined 2013, "Magneto hydrodynamic (MHD) squeezing flow of a Casson fluid between parallel disks," *academicjournals.org*, vol. 8, no. 36, pp. 1788–1799, 2013.

36. A. C.-J. of S. and Vibration and undefined 2005, "Statistical origins of fractional derivatives in viscoelasticity," *Elsevier*.

37. Y. Kawada, H. Nagahama, H. H.- Tectonophysics, and undefined 2006, "Irreversible thermodynamic and viscoelastic model for power-law relaxation and attenuation of rocks," *Elsevier*.

38. S. Mohyud-Din, M. Iqbal, S. H.- Entropy, and undefined 2015, "Modified Legendre wavelets technique for fractional oscillation equations," *mdpi.com*.

39. N. Shah, D. Vieru, C. F.-J. of M. and Magnetic, and undefined 2016, "Effects of the fractional order and magnetic field on the blood flow in cylindrical domains," *Elsevier*.

40. G. Layek, S. Mukhopadhyay, S. S.-I. communications in, and undefined 2007, "Heat and mass transfer analysis for boundary layer stagnation-point flow towards a heated porous stretching sheet with heat absorption/generation and," *Elsevier*.

41. Ahmad B., Ali Shah S. I., Ul Haq S., and Ali Shah N., "Analysis of unsteady natural convective radiating gas flow in a vertical channel by employing the Caputo time-fractional derivative," *Eur. Phys. J. Plus*, vol. 132, no. 9, Sep. 2017, https://doi.org/10.1140/EPJP/I2017-11651-1

42. H. A.-T. J. of E. and Environmental and undefined 2007, "Stagnation point flow towards a stretching surface through a porous medium with heat generation," *journals.tubitak.gov.tr*.

43. Nehad Ali Shah, Animasaun I L, Abderrahim Wakif, Koriko O K, Sivaraj R, Adegbie K S, et al, Significance of suction and dual stretching on the dynamics of various hybrid nanofluids: Comparative analysis between type I and type II models, Phys. Scr. 95 095205.

44. Nehad Ali Shah I.L. Animasaun R.O. Ibraheem H.A. Babatunde N. Sandeep and Pop I., Scrutinization of the effects of Grashof number on the flow of different fluids driven by convection over various surfaces, Journal of Molecular Liquids, Volume 249, January 2018, Pages 980–990.

45. Animasaun I. (2015) Dynamics of Unsteady MHD Convective Flow with Thermophoresis of Particles and Variable Thermo-Physical Properties past a Vertical Surface Moving through Binary Mixture. Open Journal of Fluid Dynamics, 5, 106–120. https://doi.org/10.4236/ojfd.2015.52013

46. Sowmya G., Gireesha B.J., Animasaun I.L. et al. Significance of buoyancy and Lorentz forces on water-conveying iron(III) oxide and silver nanoparticles in a rectangular cavity mounted with two heated fins: heat transfer analysis. J Therm Anal Calorim 144, 2369–2384 (2021). https://doi.org/10.1007/s10973-021-10550-7.

47. Shah N.A., Animasaun I.L., Chung J.D. et al. Significance of nanoparticle's radius, heat flux due to concentration gradient, and mass flux due to temperature gradient: The case of Water conveying copper nanoparticles. Sci Rep 11, 1882 (2021). https://doi.org/10.1038/s41598-021-81417-y PMID: 33479309

48. Hussanan Abid, Mohd Zuki Salleh Ilyas Khan, Shafie Sharidan, Convection heat transfer in micropolar nanofluids with oxide nanoparticles in water, kerosene and engine oil, Journal of Molecular Liquids 229 (2017) 482–488.

49. Aman S., Ilyas Khan., Ismail Z. et al. Heat transfer enhancement in free convection flow of CNTs Maxwell nanofluids with four different types of molecular liquids. *Sci Rep* 7, 2445 (2017). https://doi.org/10.1038/s41598-017-01358-3 PMID: 28550289

50. Khan N.S.; Gul T.; Islam S.; Ilyas Khan.; Alqahtani A.M.; Alshomrani A.S. Magnetohydrodynamic Nanoliquid Thin Film Sprayed on a Stretching Cylinder with Heat Transfer. *Appl. Sci.* 2017, 7, 271. https://doi.org/10.3390/app7030271.

51. Sheikholeslami M., Shah Z., Shafee A., Ilyas Khan et al. Uniform magnetic force impact on water based nanofluid thermal behavior in a porous enclosure with ellipse shaped obstacle. *Sci Rep* 9, 1196 (2019). https://doi.org/10.1038/s41598-018-37964-y PMID: 30718893

52. Aaiza G., Ilyas Khan & Shafie S. Energy Transfer in Mixed Convection MHD Flow of Nanofluid Containing Different Shapes of Nanoparticles in a Channel Filled with Saturated Porous Medium. *Nanoscale Res Lett* 10, 490 (2015). https://doi.org/10.1186/s11671-015-1144-4 PMID: 26698873

53. Hussanan A., Ismail Z., Ilyas Khan et al. Unsteady boundary layer MHD free convection flow in a porous medium with constant mass diffusion and Newtonian heating. *Eur. Phys. J. Plus* 129, 46 (2014). https://doi.org/https%3A//doi.org/10.1140/epjp/i2014-14046-x

54. C. Çelik, M. D.-J. of computational physics, and undefined 2012, "Crank–Nicolson method for the fractional diffusion equation with the Riesz fractional derivative," *Elsevier*.